

Finite Element Method for Numerical Stress Analysis of Aluminum plate

Zaigham Saeed Toor

Abstract—This research paper has performed the stress analysis of a uniformly static loaded plate of aluminum alloy AA2024-T3 from both ends and is center drilled using ANSYS. Analytical and Numerical solutions for Stress Concentration Factor (K_t) were obtained at different aspect ratios by varying drill diameter against the plate width and thickness. It was observed that the maximum stress was generated around the corner of drill and varied inversely with the aspect ratios while the K_t was directly proportional to the aspect ratios. The analytical and numerical solutions were in close convergence with each other and the maximum error observed was 0.047% which indicated that Finite Element Analysis (FEA) using ANSYS is effective in designing aluminum components which are subjected to drilling and riveting operations.

Index Terms— Aerospace Materials, ANSYS, Finite Element Analysis, Stress Concentration

I. INTRODUCTION

The latest trend in any engineering design involves three basic solutions. First is the analytical solution which involves calculating the output of the problem as per the defined input parameters using a mathematical equation to give an exact solution. The second solution is called a numerical solution using Finite Element Methods (FEM) also called Finite Element Analysis (FEA) which involves generating a model of the problem, defining boundary conditions in terms of load, temperature, mounting etc., then meshing the model which divides the model into small elements and finally solving the model to calculate approximate solutions out of those elements which helps in better visualization and distribution of the boundary conditions on the model. The last solution involves developing a prototype of this model after good correlation is achieved between analytical and numerical solution and perform actual experiment and the results help in faster convergence to solution and engineering design[1-7].

Stress Concentration is a common engineering consideration when designing components that involve machining such as drilling, cutting and other operations. It is defined as the increase or accumulation in generated stress in a component due to a hole or irregularity which would not have been concentrated if the irregularity was absent [8-14]. It is represented mathematically in terms of Stress Concentration Factor (SCF) as shown in (1)[7, 8, 15].

$$K_t = \frac{\sigma_{\max}}{\sigma_{\text{normal}}} \quad (1)$$

Where

K_t = Stress Concentration Factor

σ_{max} = Maximum stress in the component around the irregularity

σ_{normal} = Normal stress in the component generated in absence of irregularity

The normal stress (σ) in the components is calculated from the general stress equation in which the applied force (F) on the components is divided by the cross-sectional area (A) as shown in (2)[3, 8, 15, 16].

$$\sigma = \frac{F}{A} \quad (2)$$

For a uniformly loaded plate having a width (W), which is center drilled having drill diameter (D), the SCF is represented by (3)[15].

$$K_t = 3 - 3.13\left(\frac{D}{W}\right) + 3.66\left(\frac{D}{W}\right)^2 - 1.53\left(\frac{D}{W}\right)^3 \quad (3)$$

Aluminum alloys and composites are a major material group in the aerospace and automobile industries. Their high specific strength, good corrosion resistance and ease of manufacturing help the engineers to develop many space grade structures[17-32]. In order to develop any structure machining is of prime importance and hence after machining various irregularities are introduced in the component due to which it is important to study how these irregularities can affect the stress generated in the structure before actual fabrication can be done[3, 11, 13, 33].

II. EXPERIMENTAL PROCEDURE

The first step was to calculate the analytical K_t for the plate with a circular drill from (3). The different aspect ratios in terms of thickness and width by diameter ratios used in this analytical calculation are shown in table I.

TABLE I
Aspect Ratios

(T/D)	(W/D)
0.3	5
0.5	2.5
0.7	1.6
0.9	1.25

Date received: 26 November 2019; Accepted: May 17, 2020.

Zaigham Saeed Toor is a Materials Science & Engineering graduate from Institute of Space Technology (IST), Islamabad, Pakistan and is currently pursuing a Post-Graduate degree in the same program. He is a registered engineer with Pakistan Engineering Council (PEC).
(email: zaighamtoor93@gmail.com).

For numerical solution, Static Structural Module of ANSYS Workbench® 15.0 was used in which the first step was to declare the material properties for AA2024-T3 which are shown in Table II [21, 22, 32, 33].

TABLE II
Properties of AA2024-T3 [21, 22, 32, 33]

Property	Value
Density	2.78 g/cm ³
Youngs Modulus	73100 MPa
Poisson's Ratio	0.33
Bulk Modulus	71667 MPa
Shear Modulus	27481 MPa
Tensile Yield Strength	345 MPa
Ultimate Tensile Strength	483 MPa

The next step was to generate a model of the plate and drill a hole of the required aspect ratio. This was achieved using the design modeler and the dimensions are shown in table III in which the drill diameter was varied as per the required aspect ratios in subsequent models. The model was meshed using solid brick elements which were refined near the drilled region using mesh refinement capability of the software, so the resultant mesh became triangular for accurate results as shown in fig. 1.

The meshing statistics for both the aspect ratios are shown in table IV and V.

TABLE III
Model dimensions

Dimension	Value (mm)
Length (L)	200
Width (W)	30
Thickness (T)	5
Drill diameter (D)	5.5~24

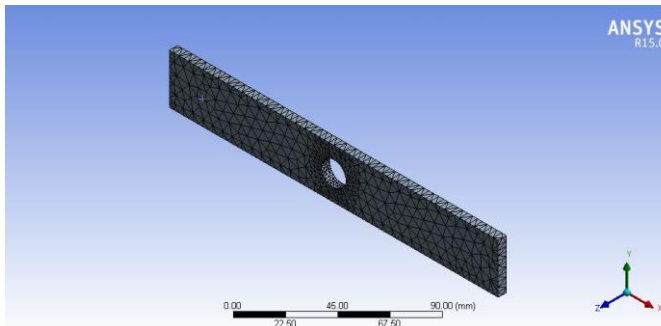


Fig 1: Meshed Aluminum Plate

TABLE IV
Meshing statistics for Thickness by Drill diameter

Aspect ratio (T/D)	Mesh type	No. of Nodes	No. of Elements
0.3	Triangular	7708	4132
0.5	Triangular	6781	3599
0.7	Triangular	6863	3679
0.9	Triangular	6114	3190

TABLE V
Meshing statistics for Width by Drill diameter

Aspect ratio (W/D)	Mesh type	No. of Nodes	No. of Elements
5	Triangular	6364	3340
2.5	Triangular	6767	3577
1.6	Triangular	8470	4632
1.25	Triangular	8660	4666

All the meshed models were subjected to the boundary conditions as shown in fig. 2. Both the ends were subjected to a static uniform loading of 250 N along the X-axis. Maximum and minimum Von-Mises stress along with total deformation were evaluated. The numerical K_t was calculated from (1). The normal stress was calculated by subtracting the drill diameter from the width of each model and multiplying it with the respective thickness of the model to get the normal area and then the applied force was divided by this area. The value of maximum stress from ANSYS was divided by this normal stress to calculate the numerical K_t .

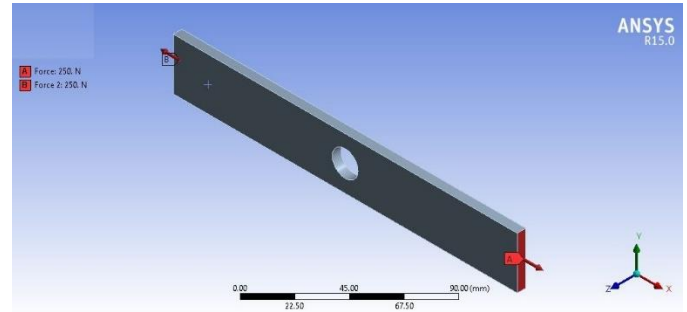


Fig 2: Boundary Conditions used

For analyzing the convergence of the analytical and numerical solution, percentage error was calculated by subtracting the numerical value from the analytical value and dividing the resultant from the analytical value as shown in (4).

$$\text{Error (\%)} = \frac{\text{Analytical } K_t - \text{Numerical } K_t}{\text{Analytical } K_t} \quad (4)$$

III. RESULTS AND DISCUSSIONS

The Von-mises stress distribution and total deformation against the respective aspect ratios is shown in fig. 3 to 18. It can be seen that for all cases the maximum stress is observed at the corner region of the hole, perpendicular to the direction of application of force, while the maximum deformation is in the direction of application of the force.

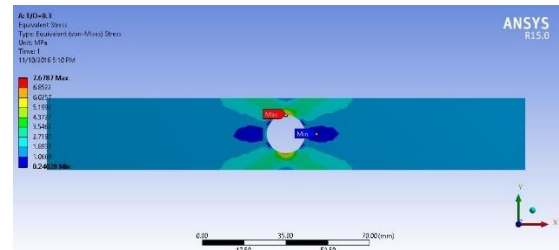


Fig 3: Stress distribution at 0.3 T/D

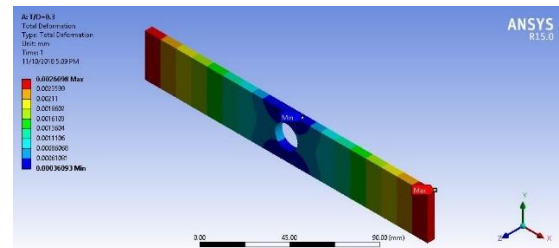


Fig 4: Total deformation at 0.3 T/D

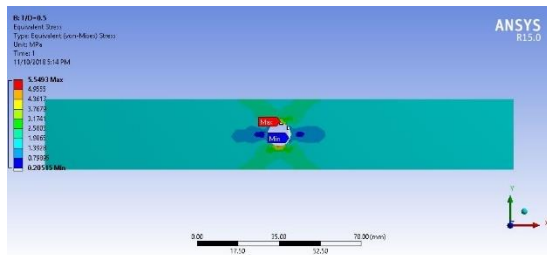


Fig 5: Stress distribution at 0.5 T/D

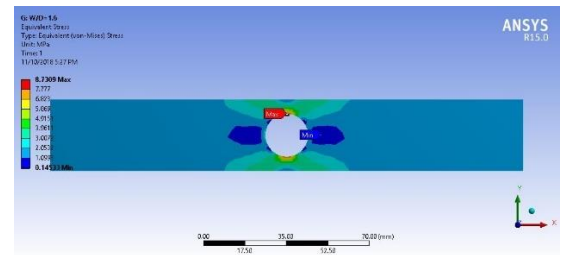


Fig 11: Stress distribution at 1.6 W/D

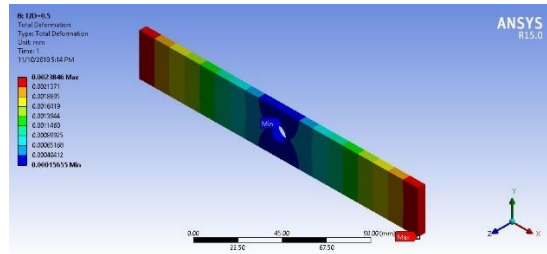


Fig 6: Total deformation at 0.5 T/D

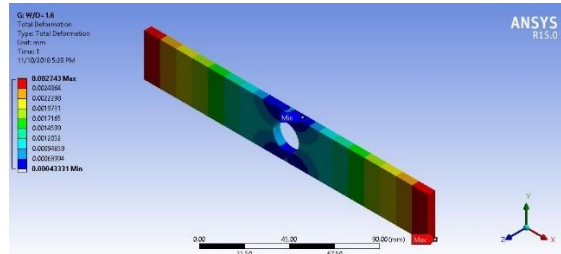


Fig 12: Total deformation at 1.6 W/D

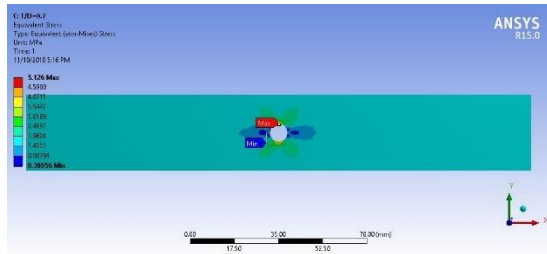


Fig 7: Stress distribution at 0.7 T/D

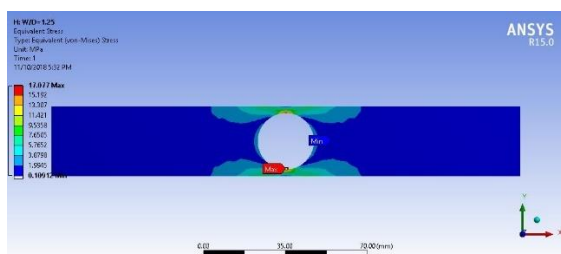


Fig 13: Stress distribution at 1.25 W/D

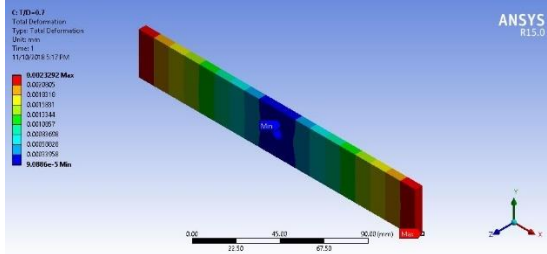


Fig 8: Total deformation at 0.7 T/D

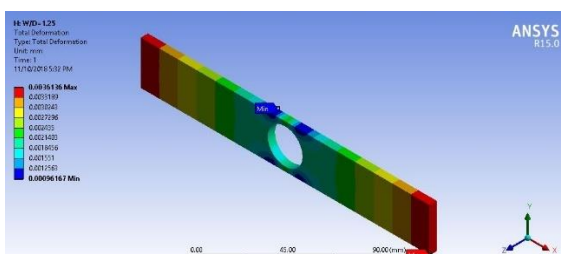


Fig 14: Total deformation at 1.25 W/D

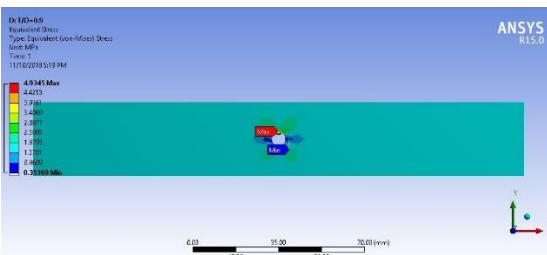


Fig 9: Stress distribution at 0.9 T/D

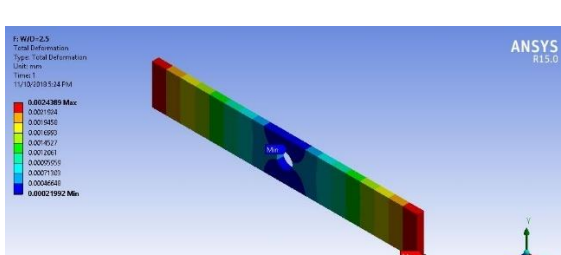


Fig 15: Total deformation at 2.5 W/D

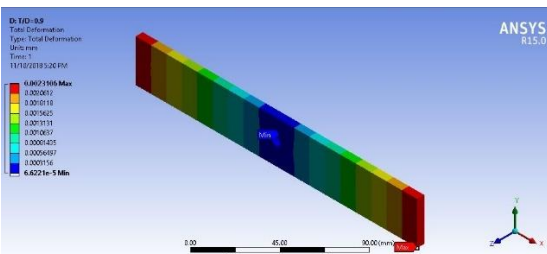


Fig 10: Total deformation at 0.9 T/D

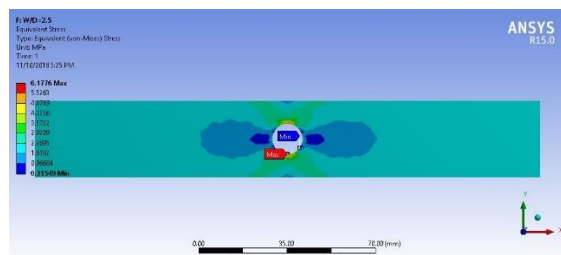


Fig 16: Stress distribution at 2.5 W/D

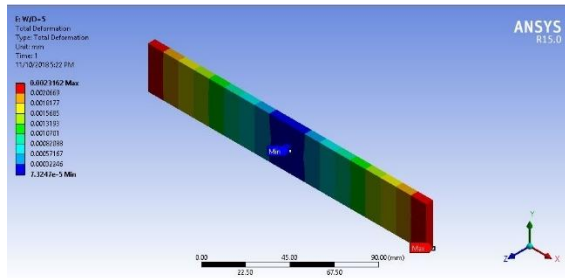


Fig 17: Total deformation at 5 W/D

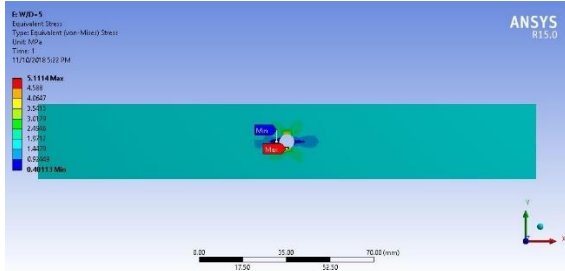


Fig 18: Stress distribution at 5 W/D

The results of analytical K_t , numerical K_t , Maximum Von-mises stress and Maximum deformation from ANSYS calculated against the respective aspect ratios, normal area and drill diameter are shown in table VI and VII respectively while fig. 19 to 24 represents their graphical representation. It can be seen in both tables and graphs that as the respective aspect ratio is increasing, both the Maximum Von-mises stress and deformation decreases, while the K_t increases. The decrease in stress and deformation can be attributed to the increase in subsequent normal area as the aspect ratio increases with the decrease in drill diameter. As the normal area increases since more material is now available to bear the load and hence less stress is generated in the plate and less stress correspondingly generates less deformation. Another significant thing observed in fig. 23 and 24 is that the analytical and numerical K_t are in good convergence with each other and the same is reflected in percentage errors of the tables irrespective of the aspect ratios

TABLE VI
Results for Aspect Ratio Thickness by Drill diameter

Diameter (mm)	16	10	7	5.5
Normal Area (mm ²)	70	100	115	122.5
Normal Stress (MPa)	3.5714	2.5	2.1739	2.0408
Aspect ratio (T/D)	0.3	0.5	0.7	0.9
Maximum Von-Mises Stress (MPa)	7.6787	5.5493	5.126	4.9345
Maximum Deformation (mm)	0.0026	0.0024	0.0023	0.0023
Numerical K_t	2.1500	2.2197	2.3579	2.4179
Analytical K_t	2.1796	2.3067	2.4495	2.5398
Error (%)	0.01358	0.0377	0.0374	0.0480

TABLE VII
Results for Aspect Ratio Width by Drill diameter

Diameter (mm)	6	12	18	24
Normal Area(mm ²)	120	90	60	30
Normal Stress (MPa)	2.0833	2.7778	4.1667	8.3333
Aspect ratio (W/D)	5	2.5	1.6	1.25
Maximum Von-Mises Stress (MPa)	5.1114	6.1776	8.7309	17.077
Maximum Deformation (mm)	0.0023	0.0024	0.0027	0.0036
Numerical K_t	2.4535	2.2239	2.0954	2.0492
Analytical K_t	2.5082	2.2357	2.1091	2.0550
Error (%)	0.0218	0.0053	0.0065	0.0028

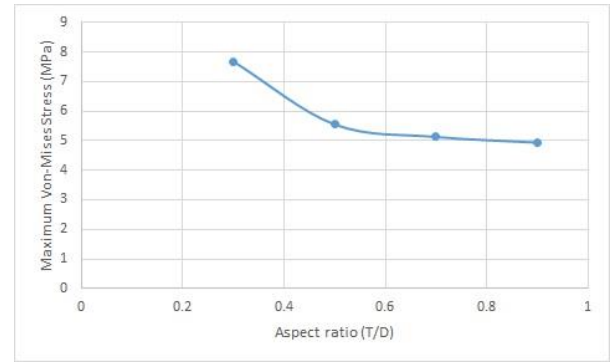


Fig 19: Effect of T/D on Von-mises stress

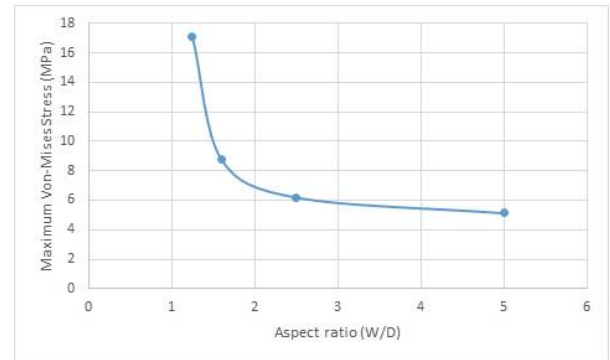


Fig 20: Effect of W/D on Von-mises stress

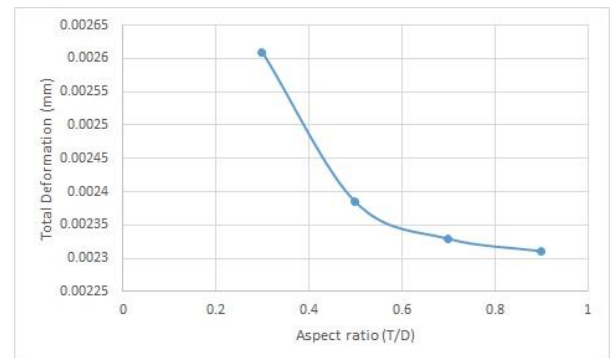


Fig 21: Effect of T/D on Deformation

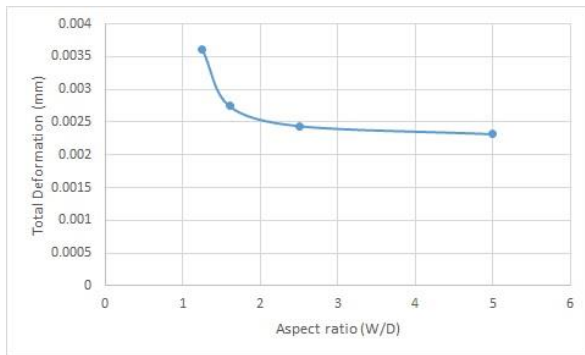


Fig 22: Effect of W/D on Deformation

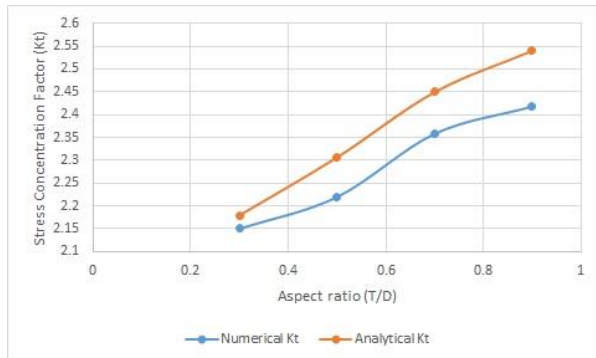


Fig 23: Effect of T/D on Analytical and Numerical Kt

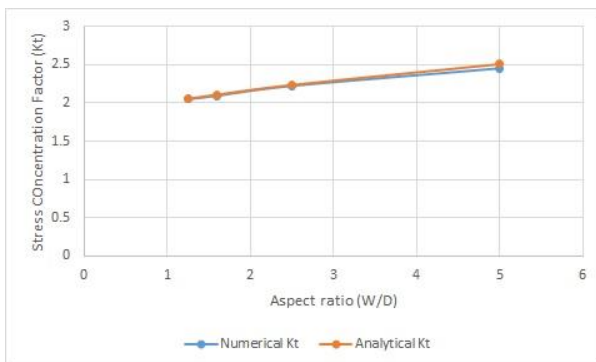


Fig 24: Effect of W/D on Analytical and Numerical Kt

IV. CONCLUSION

- The Maximum stress and deformation generated in an aluminum plate with drilled hole are inversely proportional to their respective aspect ratios
- The maximum stress generated in the plate is concentrated around the corner of drill, is perpendicular to the direction of force application and is not dependent on the aspect ratio
- Both the numerical and analytical Kt are directly proportional to the aspect ratios and were in good convergence with each other since the maximum percentage error observed was 0.047% which is very small
- FEA using ANSYS is an effective approach to design engineering components and its reliability can be verified by comparing it with its analytical solution

- The study conducted for aluminum plate can be used in aerospace, mechanical and material design of structures and wings where riveting and drilling is required

REFERENCES

- [1] M. K. Bhuariya, M. S. Rajput, and A. Gupta, "Finite Element Simulation of Impact on Metal Plate," *Procedia Engineering*, vol. 173, pp. 259-263, 2017/01/01/ 2017.
- [2] L. Engineering. (2012). *What is Von Mises Stress ?* Available: <http://www.learnengineering.org/2012/12/what-is-von-mises-stress.html>
- [3] J. Kang, W. S. Johnson, and D. A. Clark, "Three-Dimensional Finite Element Analysis of the Cold Expansion of Fastener Holes in Two Aluminum Alloys," *Journal of Engineering Materials and Technology*, vol. 124, pp. 140-145, 2002.
- [4] V. Kuppast, *FINITE ELEMENT ANALYSIS OF ALUMINIUM ALLOYS FOR THEIR VIBRATION CHARACTERISTICS* vol. 03, 2014.
- [5] D. Ngo and A. C. Scordelis, "Finite Element Analysis of Reinforced Concrete Beams," *Journal Proceedings*, vol. 64, 3/1/1967.
- [6] Z.-m. Bai, X. Wu, C.-l. Wu, and J.-x. Wang, "Quench propagation properties analysis of high-temperature superconductors using finite element method," *Physica C: Superconductivity*, vol. 436, pp. 99-102, 2006/04/15/ 2006.
- [7] A. A. Khan, M. Ahmad, and M. A. Ashraf, "Residual Life Estimation of an Attach Angle for a Cargo Aircraft," *Journal of Failure Analysis and Prevention*, vol. 16, pp. 1126 - 1133, 2016.
- [8] CORROSIONPEDIA. (2018). *Stress Concentration Factor (Kt)*. Available: <https://www.corrosionpedia.com/definition/1035/stress-concentration-factor-kt>
- [9] K. Farhangdoost and K. Aliakbari, *Comparison between Fatigue Life of Autofrettage and Nonautofrettage Cylinders Using Stress Intensity Factor (K(I))* vol. 452-453, 2010.
- [10] S. Hale. (2015). *Why Worry About Sharp Corners and Point Loads?* Available: <https://caei.com/blog/why-worry-about-sharp-corners-and-point-loads>
- [11] W. Kastner, E. Röhrich, W. Schmitt, and R. Steinbuch, "Critical crack sizes in ductile piping," *International Journal of Pressure Vessels and Piping*, vol. 9, pp. 197-219, 1981/05/01/ 1981.
- [12] R. C. Shah and A. S. Kobayashi, "Stress intensity factors for an elliptical crack approaching the surface of a semi-infinite solid," *International Journal of Fracture*, vol. 9, pp. 133-146, June 01 1973.
- [13] L. Westfall, B. J. Diak, M. A. Singh, and S. Saimoto, "Dynamic Dislocation-Defect Analysis and SAXS Study of Nanovoid Formation in Aluminum Alloys," *Journal of Engineering Materials and Technology*, vol. 130, pp. 021011-021011-7, 2008.
- [14] A. A. Khan and I. R. Memon, "Computation of Critical Crack Sizes for Crack Growth Prediction in Thin Plates," *Journal of Engineering and Applied Sciences*, vol. 23, pp. 71-77, 2004.
- [15] B. McGinty. (2018). *Stress Concentrations at Holes*. Available: <http://www.fracturemechanics.org/hole.html>
- [16] M. i. Fun. (2018). *Area of Plane Shapes*. Available: <https://www.mathsisfun.com/area.html>
- [17] M. Shifa, F. Tariq, F. Khan, Z. S. Toor, and R. A. Baloch, "Towards light weight multifunctional hybrid composite housing for satellite electronics," *Materials Research Express*, vol. 6, p. 125629, 2020/01/17 2020.
- [18] Z. S. Toor, I. Ahmed, S. Ullah, A. N. Butt, and S. W. Hussain, "Influence of Ageing time and Stress on Corrosion behavior of AA2024-T6 in saturated NaCl Solution," *Journal of Space Technology (JST)*, vol. 8, pp. 38-44, 2018.
- [19] Z. S. Toor, "Space Applications of Composite Materials," *Journal of Space Technology (JST)*, vol. 8, pp. 65-70, 2018.
- [20] S. Scale. (2018). *Plastic materials*. Available: <https://www.simscale.com/docs/content/simulation/model/materials/plasticMaterial.html#plastic-materials>

- [21] Metalmen. (2018). *Aluminum 1100 properties & products*. Available: <https://www.metalmensales.com/Aluminum-1100-Properties.html>
- [22] M. i. from. (2018). *1100 (Al99.0Cu, A91100) Aluminum*. Available: <https://www.makeitfrom.com/material-properties/1100-Al99.0Cu-A91100-Aluminum/>
- [23] Z. S. Toor, "Applications of Aluminum-Matrix Composites in Satellite: A Review," *Journal of Space Technology (JST)*, vol. 7, pp. 1-6, 2017.
- [24] M. Tisza, D. Budai, P. Z. Kovács, and L. Zs, "Investigation of the formability of aluminium alloys at elevated temperatures," *IOP Conference Series: Materials Science and Engineering*, vol. 159, p. 012012, 2016.
- [25] R. D. Sulamet-Ariobimo, J. W. Soedarsono, T. Sukarnoto, A. Rustandi, Y. Mujalis, and D. Prayitno, "Tensile properties analysis of AA1100 aluminium and SS400 steel using different JIS tensile standard specimen," *Journal of Applied Research and Technology*, vol. 14, pp. 148-153, 2016/04/01/ 2016.
- [26] I. Ahmed, S. Ullah, Z. S. Toor, A. Wadood, A. N. Butt, and S. W. Hussain, "Design, Fabrication and Beta testing of Four point Bend Immersion (FPBI) apparatus for the study of Stress Corrosion Cracking (SCC)," in *Student Research Paper Conference (SRPC) Institute of Space Technology (IST), Islamabad, Pakistan*, 2015, pp. 162-166.
- [27] Y. Rui, A. Subic, M. Takla, C. Wang, A. Niehoff, N. Hamann, *et al.*, *Biomimetic Design of Lightweight Vehicle Structures Based on Animal Bone Properties* vol. 633, 2013.
- [28] M. Wenzelburger, M. Silber, and D. Gadow, *Manufacturing of Light Metal Matrix Composites by Combined Thermal Spray and Semisolid Forming Process – Summary of the Current State of Technology* vol. 425, 2010.
- [29] H. J. Liu, H. Fujii, M. Maeda, and K. Nogi, "Tensile properties and fracture locations of friction-stir-welded joints of 2017-T351 aluminum alloy," *Journal of Materials Processing Technology*, vol. 142, pp. 692-696, 2003/12/10/ 2003.
- [30] J. Hirsch, *Aluminium Alloys for Automotive Application* vol. 242, 1997.
- [31] E. A. Starke and J. T. Staley, "Application of modern aluminum alloys to aircraft," *Progress in Aerospace Sciences*, vol. 32, pp. 131-172, 1996/01/01/ 1996.
- [32] A. A. S. M. Inc. *Aluminum 2024-T3*.
- [33] Y. Chen, A. H. Clausen, O. S. Hopperstad, and M. Langseth, "Stress-strain behaviour of aluminium alloys at a wide range of strain rates," *International Journal of Solids and Structures*, vol. 46, pp. 3825-3835, 2009/10/15/ 2009.